

In Situ Raman Spectroscopy of Alumina-Supported Metal Oxide Catalysts

Michael A. Vuurman[†] and Israel E. Wachs^{*}

Zettlemoyer Center for Surface Studies and Department of Chemical Engineering, Lehigh University, Bethlehem, Pennsylvania 18015 (Received: October 8, 1991)

The molecular structures of the surface overlayers of rhenium(VII) oxide, molybdenum(VI) oxide, tungsten(VI) oxide, chromium(VI) oxide, vanadium(V) oxide, niobium(V) oxide, and titanium(IV) oxide on γ -alumina were determined by in situ Raman spectroscopy under dehydrated conditions. It was found that the dehydrated surface metal oxide structures of all the systems under study, except for supported titanium oxide, are different from those under ambient condition where moisture is present on the surface. Supported molybdenum oxide, tungsten oxide, vanadium oxide, and niobium oxide show the presence of a highly distorted mono-oxo species (one M=O bond) at all loadings. At higher surface coverage these supported systems also reveal the presence of M-O-M linkages which are indicative of polymeric structures. Above ~20% metal oxide loading, monolayer coverage is exceeded and crystalline MoO₃, WO₃, V₂O₅, and Nb₂O₅ particles are found on the alumina surface together with the dehydrated surface species. Crystalline Re₂O₇ is not formed at high loadings and two slightly different surface rhenium oxide species are observed as a function of surface coverage. Both possess three terminal Re=O bonds and one bridging Re-O-Al bond. Polymeric chromium oxide surface species are observed at all loadings, 0.5-5% CrO₃/Al₂O₃, as well as for titanium oxide which also forms a surface metal oxide overlayer of polymeric species up to a loading of 17%. The polymeric titanium oxide surface species are, however, not sensitive to moisture and only possess Ti-O-Ti bonds and not Ti=O bonds. Crystalline TiO₂ (anatase) is found to be present at the alumina surface in the 17% TiO₂/Al₂O₃ sample.

Introduction

Supported metal oxides are extensively used as heterogeneous catalysts in numerous chemical processes ranging from, e.g., hydrodesulfurization, cracking, polymerization, and partial oxidation of hydrocarbons to the selective reduction of nitrogen oxides.¹ Knowledge of the local structure of the catalyst surface and insight into the factors which determine the surface structure play an important role in the further development and optimization of supported metal oxide heterogeneous catalytic systems. Characterization of the molecular structure of the supported metal oxides, however, is complicated since the supported metal oxide phase can simultaneously possess several different molecular structures as well as chemical states. Thus, useful characterization techniques, which can provide detailed information about the molecular structure of the surface metal oxide, must be capable of discriminating between these different states. To date, the characterization techniques which can provide such detailed molecular information are extended X-ray absorption fine structure (EXAFS), X-ray absorption near-edge spectroscopy (XANES), Fourier transform infrared spectroscopy (FTIR), Raman spectroscopy, and recently ⁵¹V solid-state NMR.

Raman spectroscopy has proved to be a very powerful characterization technique for obtaining detailed information about the molecular structure of the metal oxide overlayer on oxide supports. The reason is that each molecular state possesses a unique vibrational spectrum that is related to its structure. Furthermore, Raman spectroscopy is ideally suited for in situ studies because there are no inherent limitations on the temperature, pressures, or the presence of reaction gases during investigation. Recent improvement of Raman instruments through the use of triplemate spectrometers coupled to multichannel detectors and improved software has significantly enhanced the quality of the measurements.^{2,3} The various types of structural information which can be obtained from Raman spectroscopy about supported metal oxides was reviewed by Wachs et al. in 1986,³ and more recently by Stencel in a book entitled *Raman Spectroscopy for Catalysis* which gathers literature acquired from 1975 to 1988.⁴

Most of the previously reported Raman studies on supported metal oxide catalysts, however, were performed under ambient conditions, where moisture is present on the oxide support surface. The first in situ Raman study on supported metal oxides was reported by Wang and Hall for supported rhenium oxide⁵ and

by Schrader and Cheng for sulfided molybdenum oxide in 1983.⁶ Subsequent to these studies several in situ Raman studies have been reported,⁷⁻²⁶ however, the influence of hydration/dehydration still remains a source of confusion and has hampered progress in the understanding of supported metal oxide catalysts. The supported metal oxide systems studied to date with in situ Raman spectroscopy include molybdenum oxide,⁶⁻¹³ tungsten oxide,^{3,7,8,11,12,14,15} vanadium oxide,^{7,8,11,13,16-22} rhenium oxide,^{5,7,23} niobium oxide^{24,25} and nickel oxide.^{3,26} Except for the supported nickel oxide system, all of these in situ studies showed a drastic change in the Raman spectra upon dehydration. Generally, it was observed that the symmetric stretching frequency of the M=O bonds shifts upward upon dehydration. Except for the supported vanadium oxide system, which has recently been studied in detail under dehydrated conditions,^{7,8,11,13,16-22} the upward shift of the symmetric stretching mode is not well understood and has been attributed to an increase in metal oxide-support interaction and not to a change in structure. Thus, most studies concluded that the same surface metal oxide species is present under hydrated and dehydrated conditions and that under dehydrated conditions simply the water molecules are removed.

This article deals with the determination of the molecular structures of several metal oxides (rhenium(VII) oxide, chromium(VI) oxide, molybdenum(VI) oxide, tungsten(VI) oxide, vanadium(V) oxide, niobium(V) oxide, and titanium(IV) oxide) supported on γ -alumina by in situ Raman spectroscopy. The purpose of this work is to reveal the drastic structural change of the dispersed metal oxides upon dehydration and to show the effect of loading upon the dehydrated surface metal oxide structures. This study is part of a larger investigation to determine the molecular structures of supported metal oxides under dehydrated conditions as a function of oxide support, loading, presence of promoters, as well as a second surface metal oxide species.

Experimental Section

Sample Preparation. Most of the supported metal oxide catalysts were prepared by the incipient-wetness impregnation method on γ -alumina (Harshaw, ~180 m²/g). Aqueous solutions of ammonium metatungstate ((NH₄)₆H₂W₁₂O₄₀), ammonium heptamolybdate ((NH₄)₆Mo₇O₂₄·4H₂O), chromium nitrate ((Cr(NO₃)₃)₆·6H₂O), perhenic acid (HReO₄), and niobium oxalate/oxalic acid were used for the preparation of the corresponding supported metal oxide samples. After the impregnation step, the samples were dried at room temperature overnight, at 110 °C overnight and finally calcined in dry air at 500 °C. The vanadium oxide samples were prepared by impregnation with a vanadium triisopropoxide (VO(OC₃H₇)₃) solution in methanol. Due to the

^{*} To whom correspondence should be addressed.

[†] On leave from Anorganisch Chemisch Laboratorium, Universiteit van Amsterdam, Nieuwe Achtergracht 166, 1018 WV Amsterdam, The Netherlands.

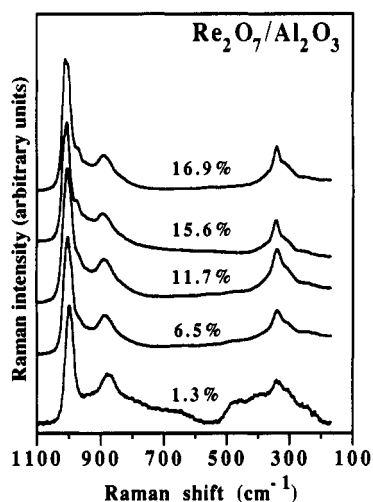


Figure 1. In situ Raman spectra of $\text{Re}_2\text{O}_7/\text{Al}_2\text{O}_3$. The rhenium oxide loading increases from 1.3 to 16.9%.

air- and moisture-sensitive nature of the alkoxide precursor, the impregnation step and subsequent drying at 350 °C were performed under a nitrogen atmosphere. The vanadium oxide samples were finally calcined in dry air at 500 °C overnight. The titanium oxide samples were prepared by impregnating the alumina support with a nonaqueous solution of $\text{Ti}[\text{OCH}(\text{CH}_3)_2]_4$ in toluene followed by drying at 110 °C and calcining at 500 °C in air overnight. All samples were recalcined for 2 h at 450 °C in dry air prior to the Raman analysis to minimize disturbing luminescence.

Raman Studies. The Raman apparatus consists of a triplemate spectrometer (Spex, Model 1877) coupled to an optical multi-channel analyzer (Princeton Applied Research, Model 1463) equipped with an intensified photodiode array detector (1024 pixels, cooled to -35 °C). In situ Raman spectra were recorded from stationary samples pressed into self-supporting wafers. A modified version of an in situ cell, developed by Wang et al.,^{5,7} was used in all the in situ experiments. In a typical experiment, the sample was heated to 500 °C in ~20 min and held for 30 min. Then the sample was cooled down to ~60 °C in ~45 min. At this temperature the in situ Raman spectrum was recorded. Ultrahigh purity hydrocarbon-free oxygen (Linde Gas) was purged through the cell during the experiment. The acquisition time used per scan was 30 s and 25 scans were averaged. The 514.5-nm line of an argon ion laser (Spectra Physics) was used as the excitation source. The laser power at the sample was 15–40 mW.

Results

The in situ Raman spectra of the supported metal oxide systems are presented in Figures 1–9. γ -Alumina does not show any Raman features in the 100–1100- cm^{-1} region and, therefore, all the observed Raman bands are assigned to metal oxide vibrations. At very low metal oxide loadings (0.7–5 wt % metal oxide), however, additional weak Raman bands are observed at ~650, ~480, and ~400 cm^{-1} in the in situ Raman spectra of all supported metal oxide samples under study which are attributed to detector noise.

$\text{Re}_2\text{O}_7/\text{Al}_2\text{O}_3$. The in situ Raman spectra of the $\text{Re}_2\text{O}_7/\text{Al}_2\text{O}_3$ catalysts as a function of rhenium oxide surface coverage are presented in Figure 1. To underline the spectral differences with increasing loading, the Raman spectra of the 1.3 and 16.9% $\text{Re}_2\text{O}_7/\text{Al}_2\text{O}_3$ samples are shown enlarged in the 1100–700- cm^{-1} range in Figure 2. One surface species, observed at all coverages, possesses bands at 1004, 890, and 340 cm^{-1} (with a shoulder at ~310 cm^{-1}). A second surface species is present at higher loadings with bands at 1015 and ~980 cm^{-1} and probably the same mode at 340 cm^{-1} (with a shoulder at ~310 cm^{-1}) since no changes are observed in the low-wavenumber region with increasing loading.

$\text{Cr}_2\text{O}_3/\text{Al}_2\text{O}_3$. The in situ Raman spectra of a series of chromium oxide on alumina are presented in Figure 3 as a function of the chromium oxide coverage. All samples (0.5–5% $\text{Cr}_2\text{O}_3/\text{Al}_2\text{O}_3$) reveal the same Raman bands at 1005, ~935 (shoulder), 880,

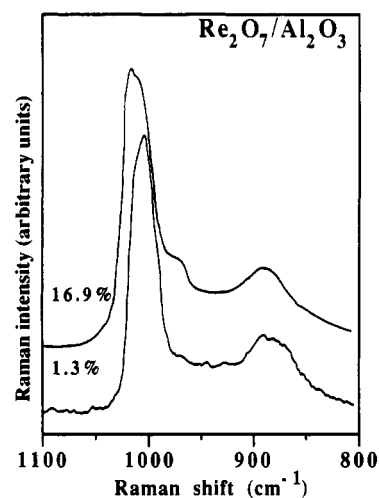


Figure 2. Enlarged presentation of the in situ Raman spectra of 1.3 and 16.9% $\text{Re}_2\text{O}_7/\text{Al}_2\text{O}_3$.

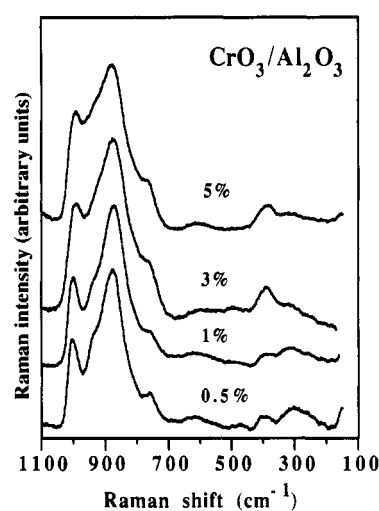


Figure 3. In situ Raman spectra of $\text{Cr}_2\text{O}_3/\text{Al}_2\text{O}_3$. The chromium oxide loading increases from 0.5 to 5%.

~760 (shoulder), ~600, 400, and ~300 cm^{-1} . The intensities of these bands do not change with increasing coverage which indicates that all these Raman bands belong to one type of surface chromium oxide species. The complete absence of Raman bands at 550 cm^{-1} (characteristic of crystalline Cr_2O_3) or at 975 and 495 cm^{-1} (characteristic of crystalline CrO_3) reveals that the chromium oxide is present as a two-dimensional overlayer up to 5 wt %.²⁷

$\text{MoO}_3/\text{Al}_2\text{O}_3$. The in situ Raman spectra of $\text{MoO}_3/\text{Al}_2\text{O}_3$ as a function of molybdenum oxide loading are presented in Figure 4. At all loadings a surface molybdate species is observed which exhibits one sharp band in the Mo=O stretching region at ~1000 cm^{-1} and a weak band in the bending region at ~300 cm^{-1} . This sharp band shifts from 993 to 1002 cm^{-1} with increasing molybdenum oxide loading and is not related to any of the other bands present in the 800–950- cm^{-1} region since at low loading only this sharp band is observed in the high-wavenumber region. A second surface molybdate species is observed in the samples with a molybdenum oxide content of 5% and higher. This species has a broad band at ~870 cm^{-1} and becomes more pronounced with increasing coverage. The Raman spectra of crystalline heptamolybdate, $(\text{NH}_4)_6\text{Mo}_7\text{O}_{24}\cdot 2\text{H}_2\text{O}$, 20% $\text{MoO}_3/\text{Al}_2\text{O}_3$ (ambient conditions) and 20% $\text{MoO}_3/\text{Al}_2\text{O}_3$ (in situ dehydrated conditions) are compared in Figure 5. The Raman spectra of $\text{MoO}_3/\text{Al}_2\text{O}_3$ under ambient conditions have been reported before and it was argued that at high loadings the surface molybdate possesses an octahedral coordinated structure which best matches that of the hydrated hepta- or octamolybdate cluster.^{4,9,28} The broad Raman band at ~870 cm^{-1} was accordingly assigned to the asymmetric

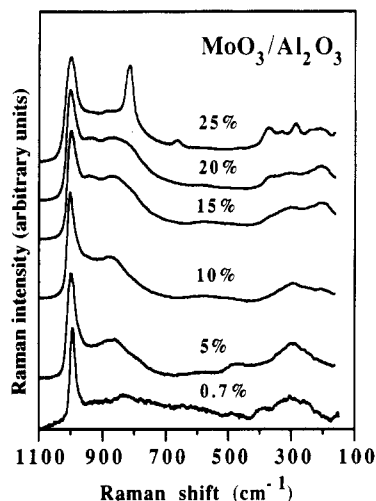


Figure 4. In situ Raman spectra of MoO₃/Al₂O₃. The molybdenum oxide loading increases from 0.7 to 25%.

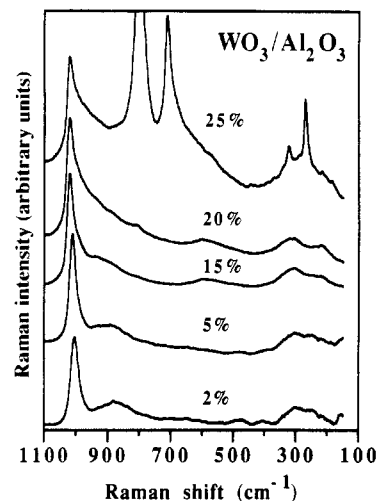


Figure 6. In situ Raman spectra of WO₃/Al₂O₃. The tungsten oxide loading increases from 2 to 25%.

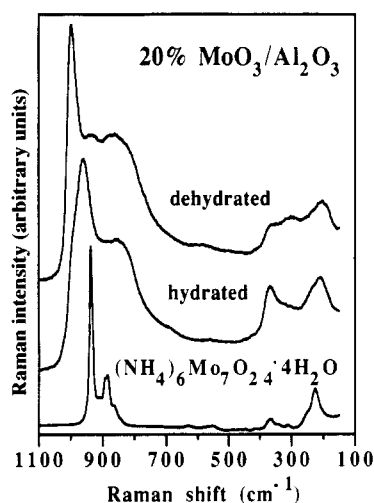


Figure 5. Raman spectra of crystalline (NH₄)₆Mo₇O₂₄·4H₂O, 20% MoO₃/Al₂O₃ (ambient condition) and 20% MoO₃/Al₂O₃ (dehydrated condition).

stretching mode of the Mo–O–Mo bonds. Comparing the intensity ratio of the 960-cm⁻¹ band relative to the 870-cm⁻¹ mode in the spectrum of crystalline (NH₄)₆Mo₇O₂₄·2H₂O versus the intensity ratio in the spectrum of the hydrated 20% sample, however, shows that the 870-cm⁻¹ band is too intense to be attributed to the asymmetric stretching mode only. Upon dehydration the broad 870-cm⁻¹ band does not change and is therefore assigned to a molybdate species that is not influenced by the presence of moisture. The in situ Raman spectra of the 10, 15, and 20% MoO₃/Al₂O₃ samples reveal the existence of a third surface molybdate species due to the presence of additional weak bands at ~940, ~580, ~360, and ~208 cm⁻¹. Above 20% MoO₃/Al₂O₃, monolayer coverage has been exceeded and crystalline MoO₃ particles are present on the dehydrated alumina surface (major bands at 815, 663, 335, and 281 cm⁻¹) together with the dehydrated surface molybdate species.

WO₃/Al₂O₃. The in situ Raman spectra of the WO₃/Al₂O₃ catalysts, as a function of tungsten oxide loading are presented in Figure 6. All spectra reveal a sharp band in the W=O stretching region, which shifts from 1004 to 1020 cm⁻¹ with increasing surface coverage, together with a broad band in the bending region at ~300 cm⁻¹. It is not very clear if this sharp band is associated with the broad band at ~880 cm⁻¹; however, the in situ Raman spectra of WO₃/SiO₂ and WO₃/TiO₂^{16,29} reveal the same sharp band up to monolayer coverage but without the presence of the broad 880-cm⁻¹ band. Accordingly, both bands are assigned to two different surface tungsten oxide species. At higher tungsten oxide loadings (15 and 20% WO₃/Al₂O₃), the

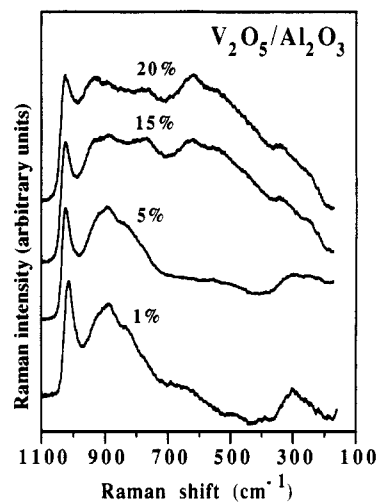


Figure 7. In situ Raman spectra of V₂O₅/Al₂O₃. The vanadium oxide loading increases from 1 to 20%.

Raman spectra reveal additional weak bands at ~940, ~590, and 215 cm⁻¹. Above 20% WO₃/Al₂O₃, the monolayer has been exceeded and crystalline WO₃ particles (major bands at 808, 711, 321, and 273 cm⁻¹) are observed on the dehydrated alumina surface together with the dehydrated surface tungsten oxide species.

V₂O₅/Al₂O₃. Figure 7 reveals the in situ Raman spectra of V₂O₅/Al₂O₃ as a function of the vanadium oxide coverage. At all loadings a surface vanadium oxide is observed which exhibits a single sharp band at 1015 cm⁻¹ which shifts to 1025 cm⁻¹ with increasing surface coverage. This band is not related to any other bands in the 800–1000-cm⁻¹ region since the intensity ratio of these bands changes with increasing loading, while on silica the sharp band has been observed without the presence of any other bands.^{18,21} A second vanadium oxide species possesses a broad band at 885 cm⁻¹, together with a shoulder at 845 cm⁻¹, and becomes more pronounced with increasing surface coverage. At 15% V₂O₅/Al₂O₃ and above, the 885-cm⁻¹ band shifts to ~925 cm⁻¹ and additional bands at ~770, ~620, ~560, ~340, and ~250 cm⁻¹ show up. Above 20% V₂O₅/Al₂O₃, monolayer coverage has been exceeded and crystalline V₂O₅ particles are also present on the dehydrated alumina surface (not shown in Figure 6).

Nb₂O₅/Al₂O₃. The in situ Raman spectra of Nb₂O₅/Al₂O₃ as a function of niobium oxide coverage are presented in Figure 8. The 3% Nb₂O₅/Al₂O₃ sample shows bands at 980, 940, 880, 630, and ~300 cm⁻¹. With increasing loading, the 980-cm⁻¹ band shifts to 988 cm⁻¹, while the 940- and 630-cm⁻¹ bands shift to ~950 and ~645 cm⁻¹, respectively, and become more pronounced

TABLE I: Raman Band Positions (in cm^{-1}) of Several Rhenium Oxide Reference Compounds

ReO_4^- (aq) (ref 34)	NaReO_4 (ref 35)	ReO_3F^a (ref 38)	ReO_3Cl^a (ref 38)	ReO_3Br^a (ref 38)	$\text{ReF}_3\text{O}_2^{a,b}$ (ref 39)	$\alpha\text{-Li}_6\text{ReO}_6$ (ref 36)	Re_2O_7 (gas) (ref 37)	assignment
971	963	1009	1001	997	1026	680	1009	$\nu_s(\text{ReO})$
916	928	980	961	963	990	505	972	$\nu_{as}(\text{ReO})$
	980							
332	331	403	293	350	370	360	341	$\delta_s(\text{OReO})$
332	331	321	344	332	370		322	$\delta_{as}(\text{OReO})$
							456	$\nu_s(\text{ReORe})$
							185	$\delta(\text{ReORe})$

^a Only the rhenium oxide vibrations are shown. ^b Wagging and rocking modes are omitted.

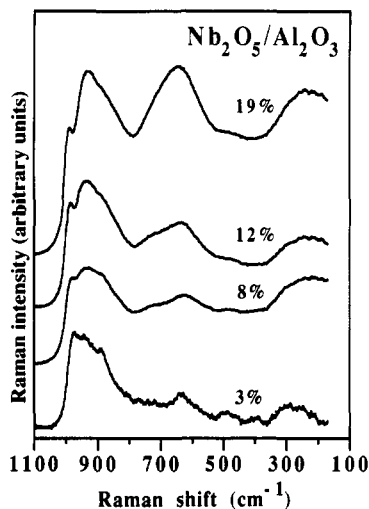


Figure 8. In situ Raman spectra of $\text{Nb}_2\text{O}_5/\text{Al}_2\text{O}_3$. The niobium oxide loading increases from 3 to 19%.

relative to the 988-cm^{-1} band. The intensity changes of the Raman bands suggest that different surface niobium oxide species are present as a function of the loading. Above 19% $\text{Nb}_2\text{O}_5/\text{Al}_2\text{O}_3$ the monolayer has been exceeded and crystalline Nb_2O_5 is present on the surface (major band at 680 cm^{-1} , not shown in Figure 8 but presented in refs 24 and 25).

$\text{TiO}_2/\text{Al}_2\text{O}_3$. Figure 9 shows the in situ Raman spectra of titanium oxide supported on alumina as a function of the surface coverage. The Raman spectra of the 5 and 13.5% $\text{TiO}_2/\text{Al}_2\text{O}_3$ samples exhibit a broad band in the $800\text{--}900\text{-cm}^{-1}$ region and two bands at ~ 710 and $\sim 460\text{ cm}^{-1}$. At 17%, the monolayer has been exceeded and crystalline TiO_2 (anatase) particles are present on the alumina surface (major bands at $643, 520, 394, 199$ and 144 cm^{-1}).³⁰

Discussion

Recently, Deo and Wachs proposed a model to predict the molecular structures of surface metal oxide species on different oxide supports (MgO , Al_2O_3 , ZrO_2 , TiO_2 , and SiO_2) under ambient conditions.³¹ It was found that under ambient conditions the support surface is hydrated and that the surface metal oxide is basically in an aqueous medium. Therefore, the hydrated surface metal oxide structures are similar to the structures observed in aqueous solutions. The hydrated surface metal oxide molecular structures were found to be dependent on the net pH at which the surface possesses zero surface charge. The net pH at point of zero charge is determined by the combined pH of the oxide support and the metal oxide overlayer. The adsorbed moisture, present under ambient condition, desorbs upon heating and the surface metal oxide overlayer becomes dehydrated. As a consequence of the model proposed by Deo and Wachs, the molecular structures of the surface metal oxide phases must generally be altered upon dehydration since the surface pH can only exert its influence via an aqueous environment. This has been experimentally confirmed by the present in situ Raman investigation as will be discussed below for the supported systems under study.

$\text{Re}_2\text{O}_7/\text{Al}_2\text{O}_3$. Under ambient conditions one hydrated rhenium oxide structure (ReO_4^-) has been reported to exist on the alumina

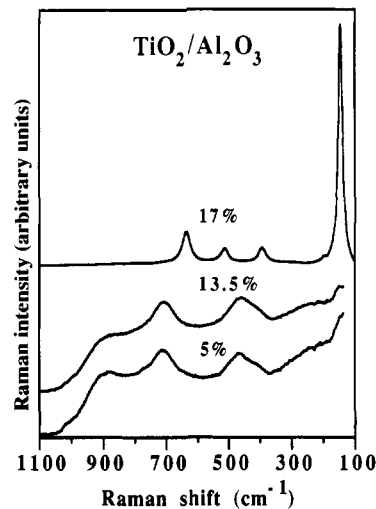


Figure 9. In situ Raman spectra of $\text{TiO}_2/\text{Al}_2\text{O}_3$. The titanium oxide loading increases from 5 to 17%.

surface independent of loading or support type.^{5,32,33} However, the present Raman study reveals that two surface rhenium oxide species are present under dehydrated conditions. One species is observed at all coverages and possesses bands at $1004, 890,$ and 340 cm^{-1} (with a shoulder at $\sim 310\text{ cm}^{-1}$), while a second species is present at higher loadings with bands at 1015 and $\sim 980\text{ cm}^{-1}$ and probably the same mode at 340 cm^{-1} (with shoulder at $\sim 310\text{ cm}^{-1}$). These findings are consistent with an earlier in situ Raman study by Wang et al.⁵ and are also supported by in situ IR spectroscopy.^{5,33}

The Raman spectra of various rhenium oxide compounds have been reported in the literature and are summarized in Table I. The table shows characteristic bands for ReO_4^- (aq),³⁴ NaReO_4 ,³⁵ $\alpha\text{-Li}_6\text{ReO}_6$,³⁶ Re_2O_7 (g),³⁷ ReO_3Z^n (with Z is F, Cl, Br),³⁸ and ReO_3F_2 .³⁹ The high-wavenumber positions of the 1004- and 1015-cm^{-1} bands in the spectra of the supported rhenium oxide catalysts reveal a tetrahedral coordination of the rhenium cation in both surface species since vibrations of octahedrally coordinated rhenium oxides are found at much lower frequencies (see Table I). The tetrahedral coordination of the rhenium cation at low surface coverage is further supported by an earlier in situ XANES study.³² For a tetrahedrally coordinated rhenium oxide, the symmetric stretching mode is always observed as a sharp and intense band in the Raman spectrum and is found at higher frequency than the weak and broad asymmetric mode.⁴⁰ Accordingly, the intense band at 1004 cm^{-1} and weak broad band at 890 cm^{-1} are assigned to the symmetric and asymmetric stretching modes of the first surface rhenium oxide species, while the 1015- and $\sim 980\text{-cm}^{-1}$ bands are assigned to the symmetric and asymmetric stretching modes of the second surface species, respectively.

The two 1004- and 1015-cm^{-1} bands are both Raman active and IR allowed (see ref 5) which indicates a symmetry lower than T_d (e.g., C_{3v} or C_{2v} symmetry). For a surface rhenium oxide species with three equivalent terminal $\text{Re}=\text{O}$ bonds and one bridging $\text{Re}-\text{O}-\text{Al}$ bond the symmetry should be C_{3v} . Rhenium oxide reference compounds with C_{3v} symmetry are, e.g., ReO_3Z^n (with Z is F, Cl, Br) (Table I). When two oxygens atoms bridge

TABLE II: Raman Band Positions (in cm^{-1}) of Several Chromium Oxide Reference Compounds

$\text{CrO}_4^{2-}(\text{aq})$ (ref 43)	$\text{CsCrO}_3\text{Br}^a$ (ref 45)	$\text{CrO}_2\text{Cl}_2^a$ (ref 46)	$\text{K}_2\text{Cr}_2\text{O}_7$ (ref 44)	$\text{K}_2\text{Cr}_3\text{O}_{10}$ (ref 44)	$\text{Cs}_2\text{Cr}_4\text{O}_{13}$ (ref 44)	CrO_3 (ref 44)	assignment
		994		980	978	1001	$\nu_{\text{as}}(\text{CrO}_2)$
		984		945	961	975	$\nu_{\text{s}}(\text{CrO}_2)$
884	955		945	930	945		$\nu_{\text{as}}(\text{CrO}_4)/\nu_{\text{as}}(\text{CrO}_3)$
	947						
	933						
847	908		902	903	904		$\nu_{\text{s}}(\text{CrO}_4)/\nu_{\text{s}}(\text{CrO}_3)$
			770	818	840		$\nu_{\text{as}}(\text{CrOCr})$
				761	831		
					719		
					560		
			560	562	512	563	$\nu_{\text{s}}(\text{CrOCr})$
				518	485	497	
		357		378	378	404	$\delta(\text{CrO}_2)$
					343		
368	242		370	358	316		$\delta(\text{CrO}_4)/\delta(\text{CrO}_3)$
348	369						
	360						
			217	262	247	375	$\rho(\text{CrO}_2 \text{OCrO})$
				230	224	338	$\delta(\text{OCrO})$
				212			
		211				208	$\rho(\text{CrO}_2 \perp \text{OCrO})$

^a Only the chromium oxide vibrations are shown.

to the surface and two equivalent terminal $\text{Re}=\text{O}$ bonds remain, the symmetry becomes C_{2v} . The symmetric stretching vibration of the terminal $\text{Re}=\text{O}$ bonds is generally observed at higher frequency for compounds possessing two $\text{Re}=\text{O}$ bonds (C_{2v}) than for species having three $\text{Re}=\text{O}$ bonds (C_{3v}) due to the increased bond order of the terminal $\text{Re}=\text{O}$ bonds. An example of a rhenium oxide complex with C_{2v} symmetry and two terminal $\text{Re}=\text{O}$ bonds is ReF_3O_2 (Table I). Although quite a few perhenato complexes have been reported with the perhenate coordinated to, e.g., Mn, Co, Ni, Zn, Cu, Cd, the diagnosis of perhenate coordination to the surface (C_{2v} or C_{3v}) is difficult from vibrational spectra alone.⁴¹ This is because the splitting of the asymmetric stretching mode into two bands (C_{3v}) or three bands (C_{2v}) is difficult to observe for broad bands associated with the surface species. Bearing this limitation in mind, the 1015- and $\sim 980\text{-cm}^{-1}$ bands of the second rhenium oxide surface species closely match the stretching modes of reference rhenium oxide compounds with three terminal $\text{Re}=\text{O}$ bonds such as ReO_3F and Re_2O_7 (gaseous) (Table I). The complete absence of Raman bands at $\sim 450\text{ cm}^{-1}$ and in the $200\text{--}150\text{-cm}^{-1}$ region, which are characteristic of $\text{Re}-\text{O}-\text{Re}$ linkages indicates, however, that the surface rhenium oxide is isolated. Thus, the data suggest that the second surface rhenium oxide species has three terminal $\text{Re}=\text{O}$ bonds and one $\text{Re}-\text{O}$ -support bond (C_{3v} symmetry). The slightly lower stretching mode of the first surface rhenium oxide species at 1004 cm^{-1} indicates that this species also has three terminal $\text{Re}=\text{O}$ bonds and one $\text{Re}-\text{O}$ -support bond (C_{3v} symmetry) since two terminal $\text{Re}=\text{O}$ bonds would have yielded a higher symmetric stretching mode than observed for the second surface species at 1015 cm^{-1} . The bending modes are split into two bands (340 and $\sim 310\text{ cm}^{-1}$) which is in agreement with C_{3v} symmetry.

The difference between these two surface species has recently been determined by TPR measurements and it was found that the bridging $\text{Re}-\text{O}-\text{Al}$ bond strength becomes weaker with increasing surface coverage.³³ As a consequence, the terminal $\text{Re}=\text{O}$ bond strength becomes stronger with increasing loading which is consistent with the Raman data since the $\nu_{\text{Re}=\text{O}}$ is found at higher frequency (1015 versus 1004 cm^{-1}).

$\text{CrO}_3/\text{Al}_2\text{O}_3$. In previous Raman studies on $\text{CrO}_3/\text{Al}_2\text{O}_3$, it was found that in the 0.5–5% loading range, hydrated monomers (CrO_4), and dimers (Cr_2O_7) are present under ambient conditions and that their concentration ratio is a function of the surface coverage.^{27,42} Dehydration transforms these different hydrated surface species into one type of chromium(VI) oxide species which possesses Raman bands at 1005 , 935 (shoulder), 880 , ~ 760 (shoulder), ~ 600 , 400 , and $\sim 300\text{ cm}^{-1}$.

Chromium(VI) oxide compounds prefer a tetrahedral coordination of the Cr^{6+} cation and various types of tetrahedrally coordinated chromium oxide compounds are known.⁴³ The tetrahedrally coordinated chromium cation can be monomeric (CrO_4^{2-}), dimeric ($\text{Cr}_2\text{O}_7^{2-}$), trimeric ($\text{Cr}_3\text{O}_{10}^{2-}$), and tetrameric ($\text{Cr}_4\text{O}_{13}^{2-}$) both in aqueous solution and in a crystalline lattice. The chromate ion has regular tetrahedral symmetry (T_d) in aqueous solution but in a crystalline lattice the symmetry is lower than T_d (usually C_s site symmetry). The dichromate ion contains one oxygen bound to two CrO_3 groups while in the trichromate structure two terminal CrO_3 groups are linked together by a CrO_4 group.⁴⁴ The tetrachromate ion possesses two terminal CrO_3 units linked together by a Cr_2O_7 unit and crystalline CrO_3 has a chain structure of CrO_4 tetrahedra with two terminal $\text{Cr}=\text{O}$ bonds and two bridging $\text{Cr}-\text{O}$ bonds for each Cr^{6+} cation.⁴⁴ When one oxygen atom is substituted (e.g., CrO_3Br^-) and three equivalent $\text{Cr}=\text{O}$ bonds remain, the symmetry becomes C_{3v} .⁴⁵ Substitution of two oxygen atoms lowers the symmetry to C_{2v} for which CrO_2Cl_2 is an example.⁴⁶ The characteristic Raman bands of these reference chromium(VI) oxide compounds are summarized in Table II. These Raman spectra reveal that the band position of the symmetric stretching mode (and consequently the bond strength) increases in the following order: $\nu_{\text{s}}(\text{CrOCr}) < \nu_{\text{s}}(\text{CrO}_3) < \nu_{\text{s}}(\text{CrO}_2)$. Furthermore, the $\nu_{\text{s}}(\text{CrO}_2)$ shifts to higher wave-number on passing from trichromate to crystalline CrO_3 ($945\text{--}975\text{ cm}^{-1}$, respectively) which reflects the increase in bond strength of the CrO_2 groups with polymerization. A similar effect is observed for the bridging CrOCr groups since its intense asymmetric stretching mode shifts from 818 cm^{-1} for $\text{K}_2\text{Cr}_3\text{O}_{10}$ to 894 cm^{-1} for crystalline CrO_3 .

Comparing the Raman spectra of $\text{CrO}_3/\text{Al}_2\text{O}_3$ with those of chromium oxide reference compounds reveals that under dehydrated conditions the surface chromium oxide possesses a polymeric structure. The very high frequency position of the 1005-cm^{-1} band reflects a very short chromium–oxygen bond distance and is only consistent with the symmetric stretching mode of CrO_2 units. The asymmetric stretching mode of the CrO_2 group could not be resolved in these Raman spectra, but was observed at 1030 cm^{-1} in the in situ Raman spectra of $\text{CrO}_3/\text{ZrO}_2$ and $\text{CrO}_3/\text{TiO}_2$.⁴⁷ The shoulder at $\sim 930\text{ cm}^{-1}$ is assigned to the stretching mode of the terminal CrO_3 groups while the very intense 880-cm^{-1} band together with the $\sim 760\text{-cm}^{-1}$ band are assigned to the stretching modes of the bridging CrOCr units. The weak broad band at $\sim 600\text{ cm}^{-1}$ belongs to the symmetric stretching mode of the CrOCr units, the 390-cm^{-1} band to the CrO_2 bending mode, and the weak 300-cm^{-1} band to the CrO_3 bending mode. The high-

wavenumber position of the stretching mode of the bridging CrOCr groups at 880 cm^{-1} indicates that the surface chromium oxide species possesses a rather long chain structure since this position is comparable with the $\nu_{\text{as}}(\text{CrOCr})$ of crystalline CrO_3 (observed at 894 cm^{-1} in its IR spectrum⁴⁴).

MoO₃/Al₂O₃. The MoO₃/Al₂O₃ system has been studied extensively under ambient conditions and it is now generally accepted that at low loadings a hydrated tetrahedrally coordinated MoO₄²⁻ species and at higher surface coverage hydrated hepta- or octamolybdate cluster are present.^{4,9,28} The Raman spectra reveal that under dehydrated conditions several surface molybdate species are present on the alumina surface up to monolayer coverage ($\leq 20\%$).

One surface species is observed at all loadings and possesses one sharp band at $\sim 1000\text{ cm}^{-1}$ and a weak band at $\sim 300\text{ cm}^{-1}$. The absence of bands in the Mo–O–Mo bending region ($< 250\text{ cm}^{-1}$) in the spectrum of the 0.7% MoO₃/Al₂O₃ sample indicates that this species is isolated. The presence of only one sharp band shows that this species possesses one short terminal Mo=O bond since a species with two equivalent Mo=O bonds would show at least two bands in the stretching region (symmetric stretch and antisymmetric stretch) and two inequivalent Mo=O bonds would yield at least two Mo=O stretching modes.⁴⁰ Wang et al. reported an IR band at $\sim 1008\text{ cm}^{-1}$ together with its overtone at 2008 cm^{-1} for a 4.6% MoO₃/Al₂O₃ sample under dehydrated conditions.⁷ The coincidence of the Raman band and the IR band further supports the monooxo model since a molybdate species with two Mo=O bonds would exhibit a more intense antisymmetric stretching mode of the O=Mo=O group while the Raman would show a more intense symmetric mode. The in situ Raman spectra do not give a straightforward indication if this mono-oxo species is octahedrally or tetrahedrally coordinated, however, octahedrally coordinated mono-oxo molybdate species are quite common (e.g., MoO₃), while there are no known tetrahedrally coordinated monooxo molybdate species. It is, therefore, most likely that the monooxo surface molybdenum oxide has a distorted octahedral coordination for the Mo⁶⁺ cation. Hardcastle et al. proposed the following structure for this species based upon their diatomic approximation method: a molybdenum oxide with one short Mo=O bond, one long opposing Mo–O bond, and four Mo–O bonds.⁴⁸ The slight shift of the Mo=O stretching mode of this species from 993 to 1002 cm^{-1} with increasing loadings can be caused by a decrease in the bond angle or in the bond strength of the O–Mo–O groups that bridge to the support. A decrease of the bond angle can be the result of crowding on the surface at higher surface coverage. A similar shift has been reported for bridging Si–(OH)–Si groups upon a decrease in the Si–O–Si angle.⁴⁹ A decrease of the bond strength can be due to the presence of protons coordinated to the bridging Mo–O–support oxygen atoms at higher surface coverage. The presence of such protons is supported by pyridine adsorption studies which revealed an increase of Brønsted acid sites with increasing surface coverage.⁵⁰

The second surface species, present at $\geq 5\%$, possesses a broad band at $\sim 880\text{ cm}^{-1}$ and is not affected by moisture. Hardcastle et al. argued that a band at 870 cm^{-1} is only consistent with a regular MoO₄ tetrahedron and that this band may be due to microcrystalline molybdates formed from small amounts of cationic impurities (such as K⁺, Na⁺, Ca⁺, Sr⁺, or Ba⁺).⁴⁸

The third molybdate surface species (bands at ~ 940 , ~ 580 , ~ 360 , and $\sim 210\text{ cm}^{-1}$) shows up at $\geq 15\%$ and has a three-dimensional structure which best matches the octahedrally coordinated hepta- or octamolybdate cluster. This dehydrated surface cluster is slightly different from the hydrated cluster, present under ambient conditions (bands at 960 , ~ 870 , 360 , 220 cm^{-1}), which is most probably due to the absence of coordinated water molecules.

Stencel et al. reported for the first time in situ Raman spectra of a 5 and 15% MoO₃/Al₂O₃ sample.⁹ They found a sharp band at 986 cm^{-1} and a broad band at 870 cm^{-1} for the 5% sample while the 15% sample showed a sharp band at 1006 cm^{-1} and a broad band at 870 cm^{-1} . Also Payen et al. reported a sharp band at 1000

cm^{-1} and a broad band at $\sim 840\text{ cm}^{-1}$ for a 14% sample.^{11,12} Both studies, however, assigned the sharp and broad band to the same surface molybdate species, while this study shows that the sharp and the broad band belong to different surface molybdate species. Moreover, due to the poor signal to noise ratio in the Raman spectra of these early studies, the bands of the dehydrated molybdate cluster could not be resolved. Chan et al. also reported an in situ Raman spectra of a 4.6% MoO₃/Al₂O₃ sample.⁸ This spectrum reveals bands basically the same bands as the present study (bands at 1012 , 950 , 872 , 320 , and 210 cm^{-1}) but no assignment of these bands were given.

WO₃/Al₂O₃. Under ambient conditions two hydrated surface tungsten oxide species have been reported to exist on the alumina surface.^{4,51} At low loadings a hydrated WO₄ species and at higher surface coverage a hydrated octahedrally coordinated cluster, which best matches the structure of W₁₂O₃₉, is present on the alumina surface. The Raman spectra reveal that under dehydrated conditions several surface tungsten oxide species are present with different structures than those under ambient conditions. At all loadings a tungsten oxide species is observed which exhibits a sharp band in the 1004 – 1020 cm^{-1} region. The presence of a single sharp band is consistent with a monooxo (one W=O bond) species as discussed above for the MoO₃/Al₂O₃ system. The upward shift of the W=O stretching mode with increasing surface coverage is similar as observed for the monooxo molybdate species. Wang et al. reported an IR band at $\sim 1018\text{ cm}^{-1}$ together with its overtone at 2008 cm^{-1} for a 4.8% WO₃/Al₂O₃ sample under dehydrated conditions, and the coincidence of the IR and Raman band further supports the monooxo model.⁷ Hardcastle et al. argued, based upon the diatomic approximation method, that this monooxo species is only consistent with a highly distorted octahedral coordination of the W⁶⁺ cation.⁵² A structure was proposed with one short W=O bond, one long opposing W–O bond and four W–O bonds which bridge to the alumina surface. A highly distorted octahedral tungsten oxide structure is also in agreement with an in situ XANES study by Horsley et al.⁵¹ A significant increase in the intensity of the pre-edge feature was reported on heating a 10% WO₃/Al₂O₃ sample. Generally, the pre-edge feature increases by any distortion of a regular octahedral environment since the center of inversion symmetry is removed and consequently the transitions from the 2s core orbital are no longer forbidden.

The broad band at $\sim 880\text{ cm}^{-1}$, assigned to a second tungsten oxide species is not affected by moisture since the Raman spectra of WO₃/Al₂O₃ shows the same broad band under ambient conditions.⁵¹ The position of this broad band at $\sim 880\text{ cm}^{-1}$ is too low for the symmetric stretching mode of a tetrahedrally coordinated tungstate⁵² and, therefore, the second surface tungstate species must have an octahedral coordination.

At higher tungsten oxide loadings (15 and 20% WO₃/Al₂O₃), the Raman spectra reveal additional weak bands at ~ 940 , ~ 590 , and 215 cm^{-1} which are indicative of a third surface species. Tungsten oxide reference compounds which possess bridging W–O–W groups, such as Na₂W₂O₇, K₂[W₂O₃(O₂)₄(H₂O)₂], or (NH₄)₆H₂W₁₂O₄₀, reveal bands in the 900 – 1000 cm^{-1} region (symmetric stretch), 800 – 900 cm^{-1} region (asymmetric stretch), 500 – 650 cm^{-1} region (W–O–W symmetric stretch), 300 cm^{-1} region (bending), and 150 – 250 cm^{-1} region (W–O–W bending).⁵¹ Thus, especially the bands at ~ 590 and $\sim 215\text{ cm}^{-1}$, present in the Raman spectra of the 15 and 20% WO₃/Al₂O₃ samples, are diagnostic of W–O–W linkages and indicate the presence of polytungstate species on the alumina surface at higher surface coverages. The Raman spectra do not reveal if this polymeric tungsten oxide is octahedrally or tetrahedrally coordinated since both polymeric tetrahedral and octahedral tungsten oxide reference compounds possess bands in the same region.⁵¹ However, the in situ XANES study by Horsley et al. demonstrated that the L₁ pre-edge is less pronounced at monolayer coverage (high loadings) than at low surface coverage where a highly distorted octahedrally coordinated species is present as discussed above.⁴⁵ A decrease in pre-edge intensity indicates that a less distorted octahedrally coordinated tungsten oxide species becomes more abundant with

increasing coverage and, therefore, it is suggested that the polymeric species has a slightly distorted octahedral coordination.

In situ Raman spectra of the $\text{WO}_3/\text{Al}_2\text{O}_3$ system have been reported before by Payen^{11,12,15} Chan,⁸ and Stencel¹⁴ which are consistent with our data. However, Payen and Chan did not discuss the structures of the dehydrated species or the influence of surface coverage, while Stencel used a model in which only isolated, tetrahedrally coordinated tungsten oxide species were considered. Such species are, as the current data shows, not present on the dehydrated alumina surface.

$\text{V}_2\text{O}_5/\text{Al}_2\text{O}_3$. Recently, Deo et al. revealed that under ambient conditions hydrated metavanadate species, $(\text{VO}_3)_n$, are present on the alumina surface at low surface coverage, while hydrated decavanadate clusters, $\text{V}_{10}\text{O}_{28}$, are observed at higher surface coverage.^{31,53} Under dehydrated conditions also several surface vanadium oxide species are identified as a function of the surface coverage, but with different structures than their hydrated counterparts. One species is present at all loadings and possesses sharp Raman band at $\sim 1015\text{ cm}^{-1}$. The presence of one single band indicates that this species has one short $\text{V}=\text{O}$ bond (monooxo) as discussed for the molybdate system. Wang et al. also found an IR band at 1030 cm^{-1} for a 10% $\text{V}_2\text{O}_5/\text{Al}_2\text{O}_3$ sample under dehydrated conditions which further supports the monooxo model.⁷ The high-frequency position reflects the extreme short $\text{V}=\text{O}$ bond distance which shows that the monooxo vanadate species must have a highly distorted structure, while the absence of bands in the $\text{V}-\text{O}-\text{V}$ bending region ($200\text{--}300\text{ cm}^{-1}$) in the Raman spectrum of the 1% $\text{V}_2\text{O}_5/\text{Al}_2\text{O}_3$ sample further indicates that this highly distorted vanadium oxide species is isolated. The upward shift from 1015 to 1025 cm^{-1} is similar as observed for the monooxo molybdate species. The isolated structure of this species is in agreement with an in situ EXAFS study by Yoshida et al. which showed that the $\text{V}-\text{V}$ distance is too large for $\text{V}-\text{O}-\text{V}$ linkages.⁵⁴ In situ ^{51}V NMR measurements further suggested a tetrahedral coordination of the V^{5+} cation at low surface coverage.⁵⁵ Thus, this surface monooxo species is best represented as an $\text{O}_3-\text{V}=\text{O}$ species with three oxygen atoms bridging to the support and one terminal oxygen closely bonded to the vanadium cation.⁵⁶ The same monooxo structure has been proposed by other authors for the $\text{V}_2\text{O}_5/\text{Al}_2\text{O}_3$ system^{17,20,21} and has also been identified on the surface of silica,^{18,21} titania,^{13,16,20,22} niobia,^{21,25} and zirconia²¹ under dehydrated conditions.

A second surface vanadium oxide with a band at 885 cm^{-1} and a shoulder at $\sim 845\text{ cm}^{-1}$ becomes more abundant at higher coverage as has also been found for the $\text{V}_2\text{O}_5/\text{TiO}_2$,^{13,16,20,22} $\text{V}_2\text{O}_5/\text{ZrO}_2$,²¹ and $\text{V}_2\text{O}_5/\text{Nb}_2\text{O}_5$,^{21,25} systems. The two Raman bands closely match those of crystalline $\text{Zn}_2\text{V}_2\text{O}_7$ (major bands at ~ 880 and 850 cm^{-1})⁵³ and, therefore, it is suggested that the second surface vanadium oxide species has a dimeric vanadate-type structure. This second surface vanadium oxide species becomes more polymerized at higher surface coverage as revealed by the shift of the symmetric stretching mode to 925 cm^{-1} and the appearance of additional bands at ~ 770 , ~ 620 , ~ 560 , ~ 340 , and $\sim 250\text{ cm}^{-1}$ which are characteristic for $\text{V}-\text{O}-\text{V}$ stretching ($500\text{--}800\text{ cm}^{-1}$) and $\text{V}-\text{O}-\text{V}$ bending modes ($150\text{--}300\text{ cm}^{-1}$), respectively. The presence of polyvanadate species at higher surface coverage has also been concluded by Went et al. on basis of their in situ Raman spectra,²⁰ although they argued that the average coordination of vanadium changes from 4-fold to 6-fold with increasing chain length. This is not in agreement with recent in situ ^{51}V NMR studies which suggested a tetrahedral coordination up to high surface coverage.⁵⁵

$\text{Nb}_2\text{O}_5/\text{Al}_2\text{O}_3$. The supported niobium oxide system has recently been studied by Jehng et al. in detail as a function of support type, calcination temperature, loading and dehydration.^{24,25,61} It was found that under ambient conditions hydrated hexaniobate-like surface species are present on the alumina support at low surface coverage, while $\text{Nb}_2\text{O}_5 \cdot n\text{H}_2\text{O}$, containing slightly distorted NbO_6 as well as NbO_7 and NbO_8 groups, are present at higher surface coverage.

Raman studies on various bulk niobium oxide compounds^{24,25} show that highly distorted tetrahedrally coordinated NbO_4

structures are not known while for regular tetrahedral NbO_4 structures (such as YNbO_4 , YbNbO_4), the major Raman frequencies appear in the $790\text{--}830\text{ cm}^{-1}$ region. In slightly distorted octahedral NbO_6 structures the major Raman frequencies appear in the $500\text{--}700\text{ cm}^{-1}$ region, while highly distorted octahedral NbO_6 structures show their major bands in the $850\text{--}1000\text{ cm}^{-1}$ region.

Under dehydrated conditions, the present study shows that several surface species are present as a function of the loading as indicated by the intensity changes of the Raman bands at 980 , 940 , 880 , and 630 cm^{-1} . The sharp band at $\sim 980\text{ cm}^{-1}$, present at all loadings is assigned to a highly distorted NbO_6 octahedron. This surface species has recently also been observed on silica, titania, and zirconia under dehydrated conditions.^{24,25} On the basis of the diatomic approximation method, Hardcastle et al. argued that this niobium oxide species possesses one terminal $\text{Nb}=\text{O}$ bond, since the Nb^{5+} cation cannot accommodate two terminal $\text{Nb}=\text{O}$ bonds and contain a highly distorted NbO_6 octahedral structure.⁵⁷ The monooxo model is further supported by recent Raman studies on layered niobium oxide compounds which possess layers of regular NbO_6 octahedra but terminate in highly distorted monooxo octahedron.⁵⁸⁻⁶⁰ These compounds also exhibit a Raman band at $\sim 985\text{ cm}^{-1}$ under dehydrated conditions similar to the monooxo surface species.

A second niobium oxide surface species also possesses a highly distorted octahedral coordination of the Nb^{5+} cation since its symmetric stretching mode at $\sim 880\text{ cm}^{-1}$ is similar to that found in hexaniobate compounds such as $\text{H}_x\text{Nb}_6\text{O}_{16}^{-(8-x)}$.⁶⁰ This species is only slightly affected by moisture since under ambient conditions a similar surface hexaniobate have been identified with a Raman band at $\sim 900\text{ cm}^{-1}$.⁶¹ The two Raman bands at ~ 940 and $\sim 630\text{ cm}^{-1}$ are assigned to a third surface species and are characteristic of a dehydrated niobium oxide species containing both highly and slightly distorted NbO_6 octahedral structures. These Raman bands are also observed for layered niobium oxide compounds which consist of both highly and slightly distorted NbO_6 octahedral structures connected by sharing corners.^{60,62} In addition, the shifts of Raman bands from ~ 940 to $\sim 950\text{ cm}^{-1}$ and from ~ 640 to $\sim 650\text{ cm}^{-1}$ upon approaching monolayer coverage also suggest that these two Raman bands arise from the same dehydrated surface niobium oxide species. The increase of the 650 cm^{-1} band relative to the 950 cm^{-1} band with increasing surface coverage is due to the increasing background at lower wavenumbers.

$\text{TiO}_2/\text{Al}_2\text{O}_3$. Solid titanium(IV) oxo complexes are rarely found to exhibit a true $\text{Ti}=\text{O}$ moiety. Some exceptions, however, exist such as $\text{TiO}(\text{porphyrin})$, $\text{TiO}(\text{phthalocyanine})$, $\text{TiO}(\text{edta H}_2)(\text{H}_2\text{O})$, and salts containing TiOF_5 .⁶³ These complexes show a $\nu(\text{Ti}=\text{O})$ in the $950\text{--}975\text{ cm}^{-1}$ region, while also in an acidic aqueous solutions of titanium(IV) oxide, a Raman band at $\sim 975\text{ cm}^{-1}$ was detected which was assigned to the $\text{Ti}=\text{O}$ stretching mode of TiO^{2+} species.⁶³ Most of the so-called "titanyl" compounds show broad bands near 900 cm^{-1} which are indicative of a $\text{Ti}-\text{O}-\text{Ti}$ chain network.⁶⁴ This is the situation in all oxohalides of the type TiOX_2 ($X = \text{F}, \text{Cl}, \text{Br}, \text{or I}$) and also in complexes such as $\text{TiOF}_2 \cdot \text{H}_2\text{O}$, $\text{TiOCl}_2 \cdot 2\text{py}$, and $\text{KTiO}(\text{PO}_4)$. Bridged $\text{Ti}-\text{O}-\text{Ti}$ moieties were also observed in acidic aqueous solution of TiCl_4 by Reichmann et al.⁶⁵ They reported Raman bands at 395 and 910 cm^{-1} which were assigned to the symmetric and anti-symmetric stretches of $\text{Ti}-\text{O}-\text{Ti}$ bonds. When the acid concentration was increased, new Raman bands at ~ 480 , 650 , and $\sim 930\text{ cm}^{-1}$ showed up which were also assigned to $\text{Ti}-\text{O}-\text{Ti}$ vibrations. At extremely high HCl concentrations a titanium containing oligomer, $[\text{Ti}_8\text{O}_{12}(\text{H}_2\text{O})_{24}]\text{Cl}_8 \cdot \text{HCl} \cdot 7\text{H}_2\text{O}$, was identified which revealed bands at 350 , 480 , and 910 cm^{-1} .

The in situ Raman spectra of the 5 and 13.5% $\text{TiO}_2/\text{Al}_2\text{O}_3$ samples do not reveal bands in the $950\text{--}1000\text{ cm}^{-1}$ region and this suggests that the surface titanium oxide species do not contain $\text{Ti}=\text{O}$ moieties. The broad $800\text{--}900\text{ cm}^{-1}$ band is indicative of $\text{Ti}-\text{O}-\text{Ti}$ moieties and so are the bands at 710 and 460 cm^{-1} . Thus, it is concluded that below a surface coverage of 17%, the titanium oxide forms a surface layer on alumina which has a polymeric titanium oxide structure.

These polymeric surface species differ from the other surface metal oxides discussed in this article in two ways. First, they do not possess short terminal $\text{Ti}=\text{O}$ bonds but only $\text{Ti}-\text{O}-\text{Ti}$ bonds while all the other surface metal oxide species do show the presence of short $\text{M}=\text{O}$ bonds as discussed above. Second, supported metal oxides with a high oxidation state (Re^{7+} , Cr^{6+} , Mo^{6+} , W^{6+} , V^{5+} , Nb^{5+}) are all influenced by hydration/dehydration while the $\text{TiO}_2/\text{Al}_2\text{O}_3$ system is not affected by moisture since the same Raman bands have been observed under ambient conditions.⁶⁶ Other supported metal oxides with a low oxidation state such as Ni^{2+} , Co^{2+} , Fe^{3+} , Mn^{4+} also reveal the same Raman bands under ambient and dehydrated conditions, demonstrating the insensitivity of these supported systems upon the presence of moisture.^{3,26,66}

Monolayer Coverage. The in situ Raman spectra further show that, above 20% $\text{MoO}_3/\text{Al}_2\text{O}_3$, 20% $\text{WO}_3/\text{Al}_2\text{O}_3$, 20% $\text{V}_2\text{O}_5/\text{Al}_2\text{O}_3$, 19% $\text{Nb}_2\text{O}_5/\text{Al}_2\text{O}_3$, and 13.5% $\text{TiO}_2/\text{Al}_2\text{O}_3$, the monolayer coverage has been exceeded and crystalline MoO_3 , WO_3 , V_2O_5 , Nb_2O_5 , and TiO_2 particles, respectively, are present on the dehydrated alumina surface. The same results have been obtained under ambient conditions which demonstrates that crystalline metal oxide particles are not affected by moisture in contrast to the surface metal oxide species and consequently the monolayer coverage is the same under ambient and dehydrated conditions. Crystalline Re_2O_7 is not stable at high temperatures but leaves the surface as gaseous Re_2O_7 during calcination and is, therefore, not present above monolayer coverage ($\sim 17\%$ $\text{Re}_2\text{O}_7/\text{Al}_2\text{O}_3$).³² Crystalline CrO_3 is also not found above monolayer coverage due to its instability at high temperatures but is reduced to crystalline Cr_2O_3 . Monolayer coverage, however, is reached at much higher surface coverage ($\sim 12\%$ $\text{CrO}_3/\text{Al}_2\text{O}_3$) than employed in this study.^{67,68}

Models. Thus, it is demonstrated that different surface species are present on the alumina surface under ambient and dehydrated conditions and the question remains if there is a general correlation between the hydrated and dehydrated surface structures. For the $\text{V}_2\text{O}_5/\text{Al}_2\text{O}_3$ system this correlation would result in a model that at low surface coverage the hydrated metavanadate species, $(\text{VO}_3)_m$ convert into highly distorted monooxo $\text{O}_3-\text{V}=\text{O}$ species while at higher loading hydrated decavanadate species, $\text{V}_{10}\text{O}_{28}\cdot 18\text{H}_2\text{O}$, convert into dimeric and polymeric surface vanadate species upon dehydration. On silica, however, it has been reported that the vanadium oxide only forms a surface overlayer at very low loadings and under ambient condition hydrated decavanadate clusters are found on the silica surface.⁵³ Upon dehydration, these clusters convert into highly distorted $\text{O}_3\text{V}=\text{O}$ species.^{18,21} Thus, simply correlating hydrated and dehydrated surface structures is not correct. This correlation also does not apply for the other supported metal oxide systems discussed in the present study. The $\text{MoO}_3/\text{Al}_2\text{O}_3$ system, for example, reveals the presence of hydrated MoO_4^{2-} species at low molybdenum oxide coverage under ambient conditions,^{4,9,28} while under dehydrated conditions a highly distorted monooxo species is observed on the alumina surface. The same monooxo molybdate is also observed by in situ Raman spectroscopy on the dehydrated silica surface, while under ambient conditions only hepta- or octamolybdate clusters are present.^{69,70}

Another model is to correlate the surface metal oxide structures with the support hydroxyl chemistry. IR studies have revealed that alumina possesses five different types of surface hydroxyl groups.⁷¹ For the $\text{MoO}_3/\text{Al}_2\text{O}_3$, $\text{WO}_3/\text{Al}_2\text{O}_3$, $\text{V}_2\text{O}_5/\text{Al}_2\text{O}_3$, and $\text{Nb}_2\text{O}_5/\text{Al}_2\text{O}_3$ systems it has recently been demonstrated that the so-called "basic hydroxyl groups" are titrated at low surface coverage, while at higher loadings the neutral and acid OH_{Al} groups are consumed.⁷² The Raman spectra show that these four supported systems possess a highly distorted monooxo structure (one short $\text{M}=\text{O}$ bond) at low loadings and polymeric structures at higher surface coverages. Therefore, it is suggested that the highly distorted monooxo species are associated with the replacement of the basic hydroxyl groups and the polymeric species are associated with the titration of the other alumina hydroxyl groups. Direct information about the interaction between the metal oxide species and the alumina surface, however, cannot be obtained from Raman spectroscopy since none of the Raman

spectra reveal bands of these bridging $\text{M}-\text{O}-\text{Al}$ bonds. The absence of these bands which are expected below $\sim 700\text{ cm}^{-1}$ (or anywhere in the spectrum) could be due to a (partly) ionic character of the bridging $\text{M}-\text{O}-\text{Al}$ bond. It is also possible that the $\text{M}-\text{O}-\text{Al}$ bonds are delocalized over the alumina surface.⁵⁶ The hydroxyl chemistry of the $\text{Re}_2\text{O}_7/\text{Al}_2\text{O}_3$ system is the same as for the four supported systems discussed above.^{72,73} However, titration of the neutral and acidic hydroxyl groups at higher surface coverage does not result in the formation of polymeric rhenium oxide species but leads to the presence of a second isolated rhenium oxide species which possesses a weaker $\text{Re}-\text{O}-\text{Al}$ bond.³³ Interestingly, silica only possesses one major surface hydroxyl group and recently it has been revealed that up to monolayer coverage only one isolated surface metal oxide species (Re ,³³ Cr ,⁴⁷ Mo ,⁶⁹ W ,²⁹ V ,^{18,21} Nb ^{24,25}) is present on the dehydrated silica surface.

Conclusions

The in situ Raman spectra reveal that the dehydrated surface metal oxide structures of all the systems under study, except for supported titanium oxide, are different from those under ambient condition where moisture is present on the surface. Supported molybdenum oxide, tungsten oxide, vanadium oxide, and niobium oxide show the presence of highly distorted monooxo species (one $\text{M}=\text{O}$ bond) at all loadings. At higher surface coverage these supported systems also reveal the presence of $\text{M}-\text{O}-\text{M}$ linkages which are indicative of polymeric structures. Above $\sim 20\%$ metal oxide loading, monolayer coverage is exceeded and crystalline MoO_3 , WO_3 , V_2O_5 , and Nb_2O_5 are found on the alumina surface together with the dehydrated surface species. These metal oxide crystallites are not sensitive to moisture in contrast to the surface metal oxide species. Crystalline Re_2O_7 is not formed at high loadings and two slightly different surface rhenium oxide species are observed as a function of surface coverage. Both are isolated and possess three $\text{Re}=\text{O}$ bonds and one bridging $\text{Re}-\text{O}-\text{Al}$ bond. Polymeric chromium oxide surface species are observed at all loadings, 0.5–5% $\text{CrO}_3/\text{Al}_2\text{O}_3$, as well as for titanium oxide which also forms a surface metal oxide overlayer of polymeric species up to a loading of 17%. The polymeric titanium oxide surface species are, however, not sensitive to moisture and only possess $\text{Ti}-\text{O}-\text{Ti}$ bonds and not $\text{Ti}=\text{O}$ bonds. Crystalline TiO_2 (anatase) is found to be present at the alumina surface in the 17% $\text{TiO}_2/\text{Al}_2\text{O}_3$ sample. Combining the present investigation under dehydrated conditions with earlier characterization studies under ambient conditions shows that a simple correlation between hydrated and dehydrated metal oxide species does not exist. Correlating the surface structure of metal oxides under dehydrated conditions with the support hydroxyl chemistry seems to be a better model to explain the results, although more work needs to be done to prove this model unambiguously.

Acknowledgment. We thank J. M. Jehng, G. Deo, A. M. Turek, D. S. Kim, D. J. Stufkens, and A. Oskam for useful discussions and W. K. Hall for providing the in situ cell.

Registry No. Al_2O_3 , 1344-28-1; Re_2O_7 , 1314-68-7; CrO_3 , 1333-82-0; MoO_3 , 1313-27-5; WO_3 , 1314-35-8; V_2O_5 , 1314-62-1; Nb_2O_5 , 1313-96-8; TiO_2 , 13463-67-7.

References and Notes

- (1) Thomas, C. L. *Catalytic Processes and Proven Catalysts*; Academic Press: New York, 1970.
- (2) Wachs, I. E.; Hardcastle, F. D. In *Emerging Characterization Techniques*; Horsley, J. A., Ed.; Catalytica Studies No. 4189cc; Mountain View, CA, 1989; pp 3–54.
- (3) Wachs, I. E.; Hardcastle, F. D.; Chan, S. S. *Spectroscopy* **1986**, *1*, 30.
- (4) Stencel, J. M. *Raman Spectroscopy for Catalysis*; van Nostrand Reinhold: New York, 1990.
- (5) Wang, L.; Hall, W. K. *J. Catal.* **1983**, *82*, 177.
- (6) Schrader, G. L.; Cheng, C. P. *J. Catal.* **1983**, *80*, 369.
- (7) Wang, L. Preparation and Characterization of Molybdenum-Alumina and Related Catalyst Systems. Ph.D. Dissertation, The University of Wisconsin, Milwaukee; University Microfilms International: Ann Arbor, MI, 1982.
- (8) Chan, S. S.; Wachs, I. E.; Murrell, L. L.; Wang, L.; Hall, W. K. *J. Phys. Chem.* **1984**, *88*, 5831.
- (9) Stencel, J. M.; Makovsky, L. E.; Sarkus, T. A.; De Vries, J.; Thomas, R.; Moulis, J. A. *J. Catal.* **1984**, *90*, 314.

- (10) Stencel, J. M.; Makovsky, L. E.; Diehl, J. R.; Sarkus, T. A. *J. Catal.* **1985**, *95*, 414.
- (11) Payen, E.; Kasztelan, S.; Grimblot, J.; Bonnell, J. P. *J. Raman Spectrosc.* **1986**, *17*, 233.
- (12) Payen, E.; Kasztelan, S.; Grimblot, J.; Bonnell, J. P. *J. Mol. Struct.* **1986**, *143*, 259.
- (13) Machej, T.; Haber, J.; Turek, A. M.; Wachs, I. E. *Appl. Catal.* **1991**, *70*, 115.
- (14) Stencel, J. M.; Makovsky, L. E.; Diehl, J. R.; Sarkus, T. A. *J. Raman Spectrosc.* **1984**, *15*, 282.
- (15) Payen, E.; Kasztelan, S.; Grimblot, J.; Bonnell, J. P. *Catal. Today* **1988**, *4*, 57.
- (16) Vuurman, M. A.; Wachs, I. E.; Hirt, A. M. *J. Phys. Chem.* **1991**, *95*, 9928.
- (17) Le Coustumer, L. R.; Taouk, B.; Le Meur, M.; Payen, E.; Guelton, M.; Grimblot, J. *J. Phys. Chem.* **1988**, *92*, 1230.
- (18) Oyama, S. T.; Wendt, G.; Lewis, K. B.; Bell, A. T.; Somarjai, G. J. *Phys. Chem.* **1989**, *93*, 6786.
- (19) Cristiani, C.; Forzatti, P.; Busca, G. *J. Catal.* **1989**, *116*, 586.
- (20) Went, G. T.; Oyama, S. T.; Bell, A. T. *J. Phys. Chem.* **1990**, *94*, 4240.
- (21) (a) Deo, G.; Eckert, H.; Wachs, I. E. *Prep.—Am. Chem. Soc., Div. Pet. Chem.* **1990**, *35*(1), 16. (b) Wachs, I. E. *Chem. Eng. Sci.* **1990**, *45*, 2561. (c) Wachs, I. E. *J. Catal.* **1991**, *129*, 307.
- (22) Pines, T. J.; Rochester, C. H.; Ward, A. M. *J. Chem. Soc., Faraday Trans.* **1991**, *87*(4), 653.
- (23) Williams, K. P. J.; Harrison, K. J. *Chem. Soc. Faraday Trans.* **1990**, *86*(9), 1603.
- (24) Jehng, J. M.; Wachs, I. E. *Catal. Today* **1990**, *8*, 37.
- (25) Jehng, J. M.; Wachs, I. E. *J. Phys. Chem.* **1991**, *95*, 7373.
- (26) Chan, S. S.; Wachs, I. E. *J. Catal.* **1987**, *103*, 224.
- (27) Hardcastle, F. D.; Wachs, I. E. *J. Mol. Catal.* **1988**, *46*, 173.
- (28) Williams, C. C.; Ekerdt, J. G.; Jehng, J. M.; Hardcastle, F. D.; Wachs, I. E. *J. Phys. Chem.* **1991**, *95*, 8791.
- (29) Kim, D. S.; Turek, A. M.; Wachs, I. E., to be published.
- (30) Wachs, I. E.; Hardcastle, F. D. *Proc. 9th Int. Congr. Catal.* **1988**, *3*, 1449.
- (31) Deo, G.; Wachs, I. E. *J. Phys. Chem.* **1991**, *95*, 5889.
- (32) Hardcastle, F. D.; Wachs, I. E.; Horsley, J. A.; Via, G. H. *J. Mol. Catal.* **1988**, *46*, 15.
- (33) Vuurman, M. A.; Wachs, I. E.; Stufkens, D. J.; Oskam, A. *J. Mol. Catal.*, submitted for publication.
- (34) Gonzalez-Vichez, F.; Griffith, W. P. *J. Chem. Soc., Dalton Trans.* **1972**, 1416.
- (35) Johnson, R. A.; Rogers, M. T.; Leroi, G. E. *J. Chem. Phys.* **1972**, *56*, 789.
- (36) Hauch, J.; Fadini, A. Z. *Naturforsch.* **1970**, *256*, 422.
- (37) Beattie, I. R.; Ozin, G. A. *J. Chem. Soc. (A)* **1969**, 2615.
- (38) Müller, A.; Krebs, B.; Hölting, W. *Spectrochim. Acta* **1967**, *23*, 2753.
- (39) Beattie, I. R.; Crocombe, R. A.; Ogdin, J. S. *J. Chem. Soc., Dalton Trans.* **1977**, 1481.
- (40) Nakamoto, N. *Infrared and Raman Spectroscopy of Inorganic and Coordination Compounds*, 3rd ed.; Wiley: New York, 1978.
- (41) Chakravorti, M. C. *Coord. Chem. Rev.* **1990**, *106*, 205.
- (42) Vuurman, M. A.; Stufkens, D. J.; Oskam, A.; Moulijn, J. A.; Kapteijn, F. *J. Mol. Catal.* **1990**, *60*, 83.
- (43) Michel, G.; Machiroux, R. *J. Raman Spectrosc.* **1986**, *17*, 79.
- (44) Mattes, R. Z. *Anorg. Allg. Chem.* **1971**, *362*, 163.
- (45) Müller, A.; Schmidt, K. H.; Ahlborn, E. *Spectrochim. Acta* **1973**, *29A*, 1773.
- (46) Stammreich, H.; Kawai, K.; Tavares, Y. *Spectrochim. Acta* **1959**, *438*.
- (47) Vuurman, M. A.; Wachs, I. E.; Stufkens, D. J.; Oskam, A. *J. Mol. Catal.*, submitted for publication.
- (48) Hardcastle, F. D.; Wachs, I. E. *J. Raman Spectrosc.* **1990**, *21*, 683.
- (49) Pelmenchikov, A. G.; Pavlov, V. I.; Zhidomirov, G. M.; Beran, S. *J. Phys. Chem.* **1987**, *91*, 3325.
- (50) Segawa, K.; Hall, W. K. *J. Catal.* **1982**, *76*, 89.
- (51) Horsley, J. A.; Wachs, I. E.; Brown, J. M.; Via, G. H.; Hardcastle, F. D. *J. Phys. Chem.* **1987**, *91*, 4041.
- (52) Hardcastle, F. D.; Wachs, I. E. In press.
- (53) Deo, G.; Hardcastle, F. D.; Richards, M.; Hirt, A. M.; Wachs, I. E. In *Novel Materials in Heterogeneous Catalysis*, Baker, R. T., Murrell, L. L., Eds.; ACS Symp. Ser. American Chemical Society: Washington, DC, 1990, Vol. 437, p 317.
- (54) Yoshida, S.; Tanaka, T.; Nishimura, Y.; Mizutani, H.; Funabiki, T. *Proc. 9th Int. Congr. Catal.* **1988**, *3*, 1473.
- (55) Eckert, H.; Wachs, I. E. *J. Phys. Chem.* **1989**, *93*, 6796.
- (56) Hardcastle, F. D.; Wachs, I. E. *J. Phys. Chem.* **1991**, *95*, 5031.
- (57) Hardcastle, F. D.; Wachs, I. E. *Solid State Ionics* **1991**, *45*, 201.
- (58) Jacobson, A. J.; Johnson, J. W.; Lewandowski, J. T. *Inorg. Chem.* **1985**, *24*, 3727.
- (59) Hardcastle, F. D.; Wachs, I. E.; Jacobson, A. J.; Lewandowski, J. T., unpublished results.
- (60) Jehng, J. M.; Wachs, I. E. *Chem. Mater.* **1991**, *3*, 100.
- (61) Jehng, J. M.; Wachs, I. E. *J. Mol. Catal.* **1991**, *67*, 369.
- (62) Jacobson, A. J.; Lewandowski, J. T.; Johnson, J. W. *J. Less-Common Mater.* **1986**, *116*, 137.
- (63) Grätzel, M.; Rotzinger, F. P. *Inorg. Chem.* **1985**, *24*, 2320.
- (64) Clark, R. J. H. *The Chemistry of Titanium and Vanadium*; Elsevier: Amsterdam, 1968.
- (65) Reichmann, M. G.; Bell, A. T. *Langmuir* **1987**, *3*, 111.
- (66) Wachs, I. E., to be published.
- (67) Vuurman, M. A.; Wachs, I. E. *J. Mol. Catal.*, in press.
- (68) Vuurman, M. A.; Wachs, I. E., to be published.
- (69) de Boer, M.; van Dillen, A. J.; Koningsberger, D. C.; Geus, J. W.; Vuurman, M. A.; Wachs, I. E. *Catal. Lett.* **1991**, *11*, 227.
- (70) Williams, C. M.; Ekerdt, J. G.; Jehng, J. M.; Hardcastle, F. D.; Wachs, I. E. *J. Phys. Chem.* **1991**, *95*, 8781.
- (71) Turek, A. M.; Decanio, E.; Wachs, I. E. *J. Phys. Chem.*, in press.
- (72) Boehm, H. P.; Knözinger, H. In *Catalysis—Science and Technology*; Anderson, J. R., Boudart, M., Eds.; Springer-Verlag: West Berlin, 1983; Vol. 38.
- (73) Sibeijn, M.; Spronk, R.; van Veen, J. A. R.; Mol, J. C. *Catal. Lett.* **1991**, *8*, 2.